Supporting Information

GSH/pH-Sensitive Förster Resonance Energy Transfer Nanoparticles for Synergistic Chemotherapy and Chemodynamic Therapy

Xiaodong Zheng,[a] Yingjian Cui,[a] Jianxin Rong,[a] Shengli Chen,[a] Xiongwei Qu,[a,*] Xiuli Hu[a,*]

[†] Institute of Polymer Science and Engineering, School of Chemical Engineering, Hebei University of Technology, Tianjin 300130, China;

* Corresponding authors: Prof. X. Qu (xwqu@hebut.edu.cn); Prof. X. Hu (huxiuli@hebut.edu.cn)

1. Experimental Section

1.1 Materials

Doxorubicin hydrochloride (DOX), N-(tert-Butoxycarbonyl)-N-methylglycine, 4-(1,2,2-Triphenylvinyl) phenol (TPE-OH), 4-Cyano-4-(dodecylsulfanylthiocarbonyl) sulfanylpentanoic acid (CDTCP), 1-(3-dimethylaminopropyl)-3-ethylcarbodiimide (EDC) and 3-bromo-1-propanol were purchased from Shanghai Bide Pharmaceutical Technology Co., Ltd. (Shanghai, China). Propylene oxide, triethylamine (TEA) triphosgene, 4-dimethylaminopyridine (DMAP), glutathione (GSH), 5,5'-Dithiobis (2-nitrobenzoic acid), tris(2-carboxyethyl) phosphine hydrochloride (TCEP), methylacryloyl chloride and DL-α-lipoic acid (LA) were purchased from Energy Chemistry (Anhui, China). Hexylamine and azobisisobutyronitrile (AIBN) were purchased from Shanghai Aladdin Biochemical Technology Co., Ltd. (Shanghai, China). 4T1 cells were purchased from the Cell Bank of Type Culture Collection of Chinese Academy of Sciences.

1.2 Characterization

The chemical structure was characterized using ^{1}H NMR spectroscopy (400 MHz; AVANCE 400, Bruker, Switzerland). The samples were lyophilized using a freeze dryer (FD-1A-50, Boyikang, China). Raman spectrometer (inVia Reflex, Renishaw, UK). Molecular weights and molecular weight distributions (*Đ*) were characterized using GPC (1260 Series, Agilent Technologies, USA). The particle size was measured using a dynamic light scattering instrument (Nano-ZS90, Malvern, UK). Fluorescence was determined using a fluorescence spectrometer (Spectrofluorometer FS5, Edinburgh instruments, UK). The UV absorbance of the sample was determined using a UV spectrophotometer (TU-1900, PERSEE, China). Intracellular fluorescence imaging images were captured using a confocal laser scanning microscope (LSM-900, Carl Zeiss, Germany). Cell viability staining was observed using an inverted fluorescence microscope (Evos FL Auto2, Thermo Fisher Scientific, USA). The Morphology of assembly was investigated by TEM (Talos F200S, FEI, USA).

1.3 Experimental Methods

1.3.1 Synthesis of Sarcosine N-carboxyanhydride (Sar-NCA)

N-(tert-Butoxycarbonyl)-N-methylglycine (10 g, 52.8 mmol) was dissolved in 60 mL of acetonitrile, followed by addition of propylene oxide (38.5 mL, 528 mmol). The flask was placed in an ice-water bath, then triphosgene (7.85 g, 26.4 mmol) was added, and the mixture was stirred for 1.5 hs. After the reaction, 30 mL of deionized water was added and the product was extracted with ethyl acetate. The organic phase was separated, washed three times with saturated sodium chloride solution, dried with $MgSO_4$ and recrystallized three times in n-hexane to obtain a white solid of 4.8 g with yield of 78%. The chemical structure of Sar-NCA was characterized by ^{1}H NMR (400 MHz, $CDCl_3$).

1.3.2 Synthesis of Polysarcosine (Psar)

To the solution of N-carboxyanhydride (Sar-NCA) (4 g, 34.7 mmol) in 15 mL of dry DMF, 62 μL (0.47 mmol) of n-hexylamine was added under nitrogen protection. The reaction was stirred at room temperature for 48 h. After that, deionized water was added and the mixture was dialyzed for 48 h and free-dried to obtain a white solid of 1.3 g with yield of 32.5%. The chemical structure of Psar was characterized by ^{1}H NMR (400 MHz, D_2O).

1.3.3 Synthesis of Psar macromolecular chain transfer agent (Psar-MCTA)

Psar (1.2 g, 0.221 mmol) was dissolved in 50 mL of dry DCM. Then CDTCP (0.36 g, 0.892 mmol), EDC (0.069 g, 0.44 mmol) and DMAP (0.0054 g, 0.044 mmol) were added to the solution and stirred in a nitrogen atmosphere for 24 h. After the reaction, the mixture was precipitated in diethyl ether for three times, and the resulted solid was dissolved in 10 mL of DMF and dialyzed with deionized water for 48 h, and freeze-dried to obtain 1.1 g of yellow product (yield, 85%). The chemical structure of Psar-MCTA was characterized by ^{1}H NMR (400 MHz, D_2O).

1.3.4 Synthesis of 3-(4-(1,2,2-triphenylvinyl) phenoxy) propan-1-ol (TPE-PP)

TPE-OH (0.9918 g, 2.85 mmol) was dissolved in 15 mL dry tetrahydrofuran (THF), followed by the addition of 3-bromo-1-propanol (1.59 g, 11.4 mmol) and K_2CO_3 (1.58 g, 11.4 mmol) under nitrogen atmosphere at 80 °C for 24 h. After the reaction, K_2CO_3 was filtered out and then 20 mL of deionized water was added and extracted three times with ethyl acetate. The organic phase was retained. Wash three times with saturated sodium chloride solution, dry with $MgSO_4$ and purify by column chromatography to give 0.92 g white solid, yield = 79%. The chemical structure of TPE-PP was characterized by ^{1}H NMR (400 MHz, DMSO-d_6).

1.3.5 Synthesis of 3-(4-(1,2,2-triphenylvinyl) phenoxy) propyl methacrylate (TPE-MA)

TPE-PP (0.85 g, 2.09 mmol) was dissolved in 15 mL of dry DCM followed by the addition of 585 μL of triethylamine (4.2 mmol) and slow dropwise addition of 710 μL of methacryloyl chloride (7.32 mmol) in an ice water bath for 0.5 hs. After removing from the ice bath, the mixture was stirred at room temperature for 22 h. The reaction mixture was then washed three times with saturated sodium chloride solution, dried with $MgSO_4$ and purified by column chromatography to give 0.78 g white solid, yield = 79%. The chemical structure of TPE-MA was characterized by ^{1}H NMR (400 MHz, DMSO-d_6).

1.3.6 Synthesis of Psar-b-P(LA-co-TPE)

Macromolecular chain transfer agent Psar-MCTA (100 mg, 0.0172 mmol), LA (142 mg, 0.688 mmol), TPE-MA (326 mg, 0.688 mmol), and AIBN (0.29 mg, 0.0017 mmol) were dissolved in dry DMF and stirred at 70 °C in a nitrogen atmosphere for 24 h. After the reaction, the mixture was dialyzed for 72 h, and freeze-dried to obtain light yellow product of 240 mg (yield, 42%). The chemical structure of Psar-b-P(LA-co-TPE) was characterized by ^{1}H NMR (400 MHz, DMF-d_7).

1.3.7 Preparation of Psar-b-P(LA-co-TPE) nanoparticles.

The preparation of Psar-b-P(LA-co-TPE) nanoparticles was carried out using the nanoprecipitation method. Briefly, 5 mg of Psar-b-P(LA-co-TPE) dissolved in 300 μL of DMF was slowly added dropwise to 2.5 mL of deionized water and stirred overnight. Dialyze with deionized water for 4 h to obtain Psar-b-P(LA-co-TPE) nanoparticles.

1.3.8 Preparation of Fe@NPs.

5 mg of Psar-b-P(LA-co-TPE) was dissolved in 300 μL DMF and 2.4 mg of $FeCl_3$ was dissolved in 200 μL of deionized water, respectively. The $FeCl_3$ solution was slowly added to Psar-b-P(LA-co-TPE) with stirring for 6 h, and Fe@NPs were obtained by dialysis for 4 h.

1.3.9 Preparation of DOX@FeNPs.

5 mg of Psar-b-P(LA-co-TPE) was dissolved in 300 μL DMF, and 1 mg of DOX·HCl was dissolved in 30 μL DMSO and neutralized with TEA. The two solutions were mixed and then dropwise added to 2.5 mL of deionized water with stirring. Then 200 μL $FeCl_3$ aqueous solution (12 mg/mL) was added and stirred in dark for 6 h. DOX@FeNPs were obtained by dialysis for 4 h.

The drug loading content (DLC) and drug loading efficiency (DLE) of DOX were determined by the standard curves of DOX in DMSO (Figure S10), which were plotted based on the absorption values recorded at 498 nm of different concentrations of DOX measured by UV-Vis, according to the following equations:

$$DLC\ (wt\%) = \frac{the\ weight\ of\ DOX\ in\ the\ NPs}{the\ weight\ of\ NPs} * 100\% \quad (1)$$

$$DLE\ (wt\%) = \frac{the\ weight\ of\ DOX\ in\ the\ NPs}{the\ weight\ of\ feeding\ DOX} * 100\% \quad (2)$$

1.3.10 In vitro drug release from DOX@FeNPs.

The drug release behavior of DOX@Fe NPs was studied at 37 °C. Briefly, DOX@FeNPs solution (5 mL, 3 mg/mL) was packed in a dialysis bag and immersed in 50 mL of PBS buffers with different pH values or PBS containing 5 mM glutathione (GSH). At designed intervals, 1 mL of the external solution was taken and replenished with 1 mL of fresh PBS. The absorption values of the extracted solution were measured at 498 nm to determine the DOX content. The release experiments were conducted in triplicate with standard deviations.

The cumulative drug release was calculated from the standard curve according to the following formula:

$$\text{Cumulative release (\%)} = (M_t/M_0) \times 100\% \qquad (3)$$

Where M_t is the amount of drug released at time t and M_0 is the total amount of drug in the NPs.

1.3.11 In vitro cytotoxicity study

The cytotoxicity of Psar-b-P(LA-co-TPE), DOX, Fe@NPs and DOX@FeNPs was determined using CCK-8 assay. In brief, 4T1 cells undergoing logarithmic growth phase were seeded in 96-well plates (100 μL, 5000 cells per well /well) and incubated at 37 °C overnight. Then DOX, Fe@NPs and DOX@FeNPs were added with final DOX concentrations of 0.3125, 0.625, 1.25, 2.5, 5, and 10 μg/mL, respectively. After incubation for 48 h, the medium was removed, rinsed with PBS for three times and a CCK-8 solution (100 μL, volume fraction 10%) was added to each well. After incubation for 4 h, the absorbance value was recorded at 450 nm with a microplate reader (BioTek Epoch 2, Agilent).

In vitro biocompatibility of Psar-b-P(LA-co-TPE) was measured by similar method by adding Psar-b-P(LA-co-TPE) with different concentrations into 4T1 cells seeded in 96-well plates and determined using CCK-8 assay.

1.3.12 Intracellular ROS detection.

Intracellular ROS generation was measured using 2',7'-dichlorofluorescein diacetate (DCFH-DA) as a probe. Specifically, 4T1 cells were treated with PBS, Psar-

b-P(LA-co-TPE) (5 μg/mL), Fe@NPs (5 μg/mL), DOX@Fe NPs (5 μg/mL), respectively, and then the culture medium was replaced and washed with PBS for three times. DMEM containing DCFH-DA (2 μM) was added and further incubated for 20 min in the dark and the intracellular ROS was imaged by Confocal Laser Scanning Microscopy (CLSM).

1.3.13 Intracellular FRET signal imaging.

In order to study the cellular uptake of DOX@Fe NPs and the intracellular release of DOX from DOX@Fe NPs, 4T1 cells were incubated with DOX@Fe NPs (5 μg/mL) for 2, 4, 6, 8, 10, 12 h, respectively. The culture medium was replaced and washed with PBS and fixed with paraformaldehyde for 15 min. The intracellular FRET signal was recorded by CLSM.

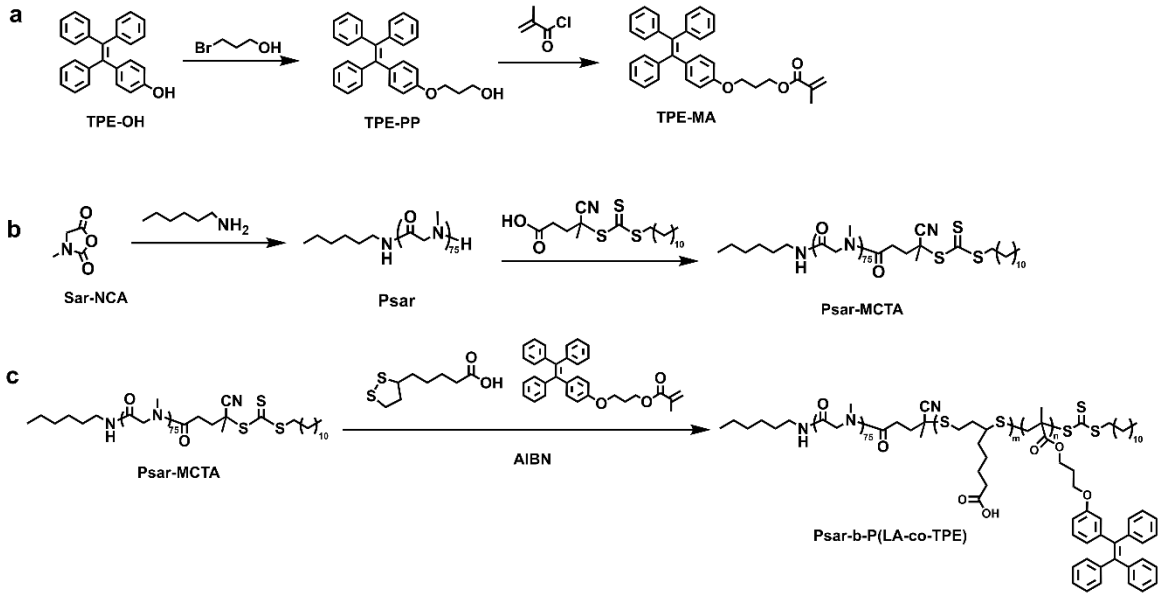

Fig. S1 Synthetic route of (a) TPE-MA; (b) Psar-MCTA; (c) Psar-b-P(LA-co-TPE).

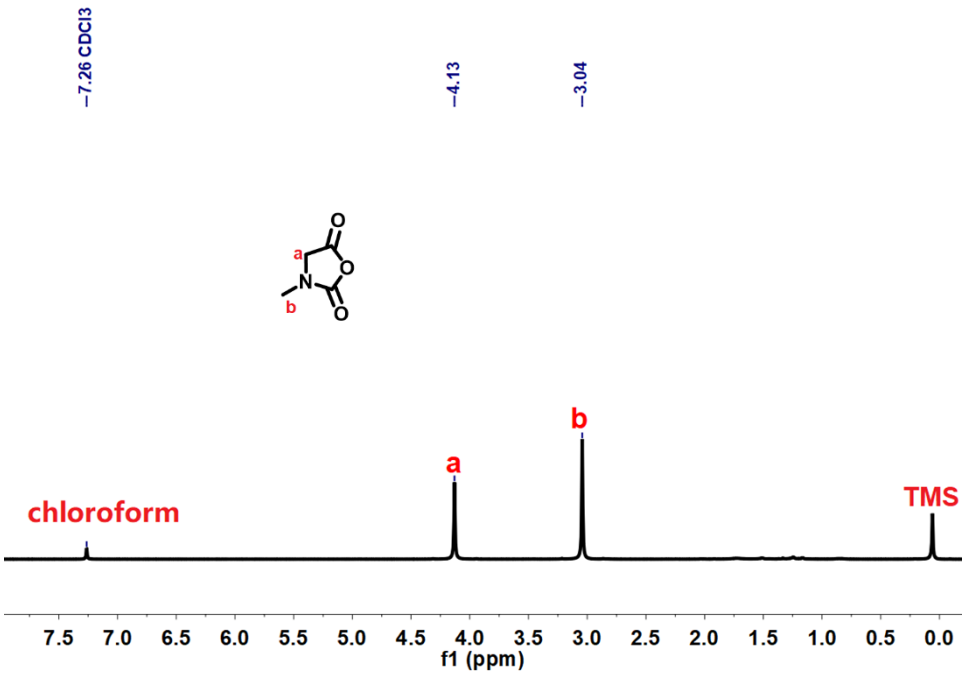

Fig. S2 ^{1}H NMR spectrum of Sar-NCA in $CDCl_3$

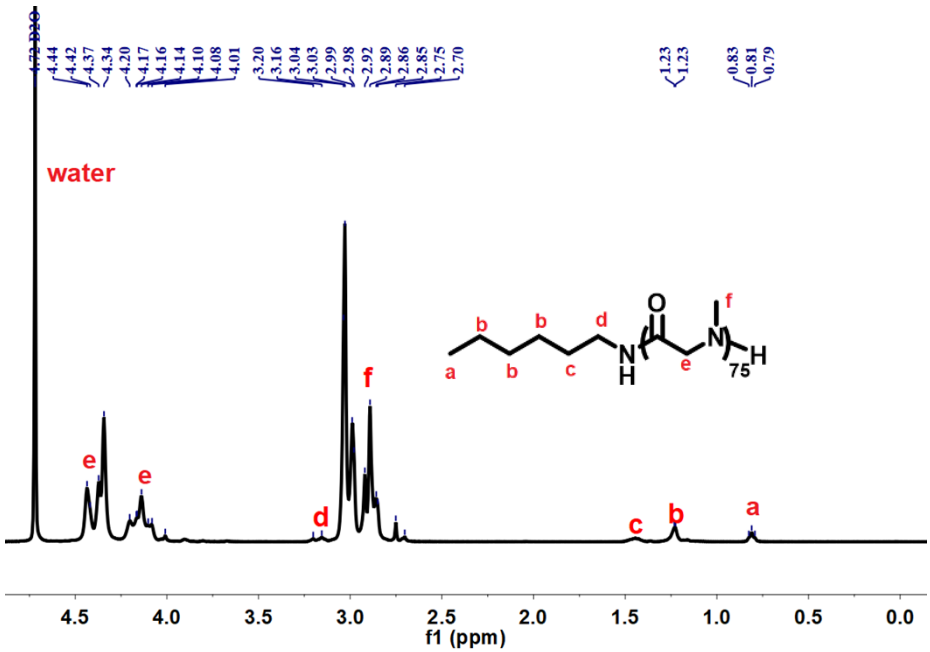

Fig. S3 ^{1}H NMR spectrum of Psar in D_2O

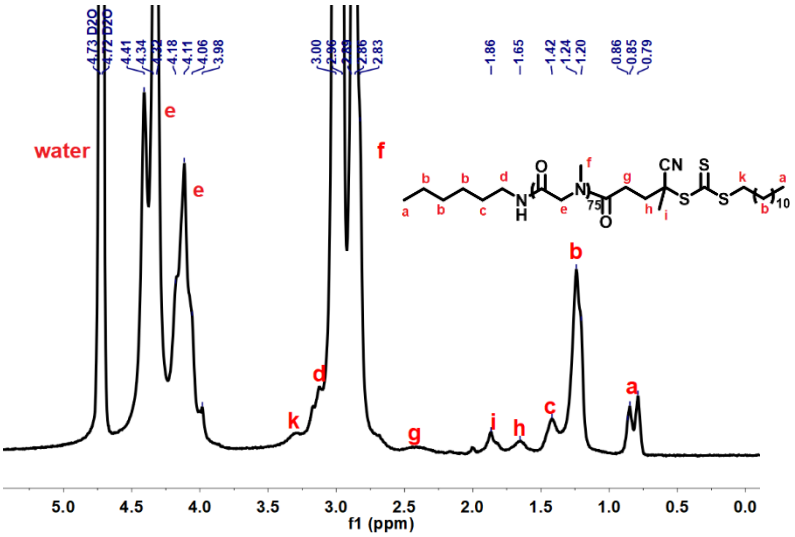

Fig. S4 ^{1}H NMR spectrum of Psar-MCTA in D_2O

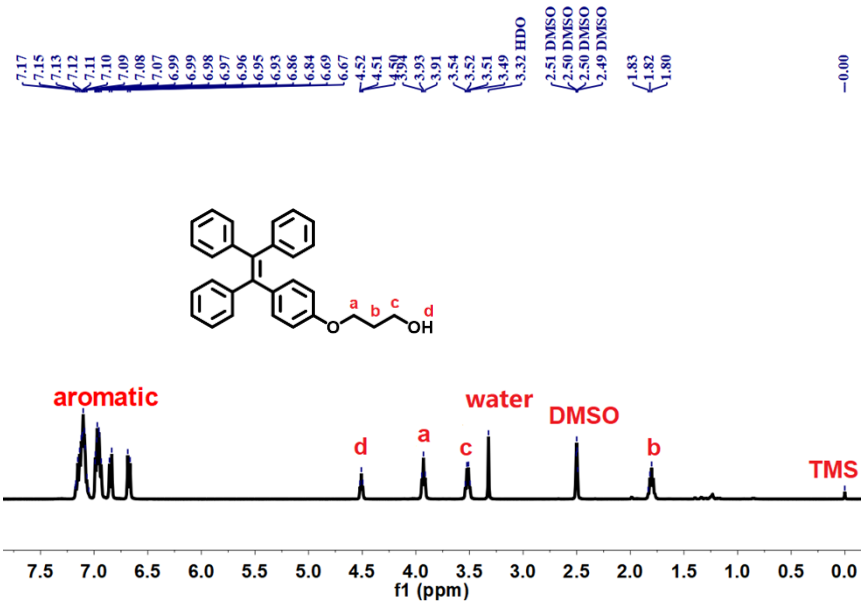

Fig. S5 ^{1}H NMR spectrum of TPE-PP in DMSO-d_6

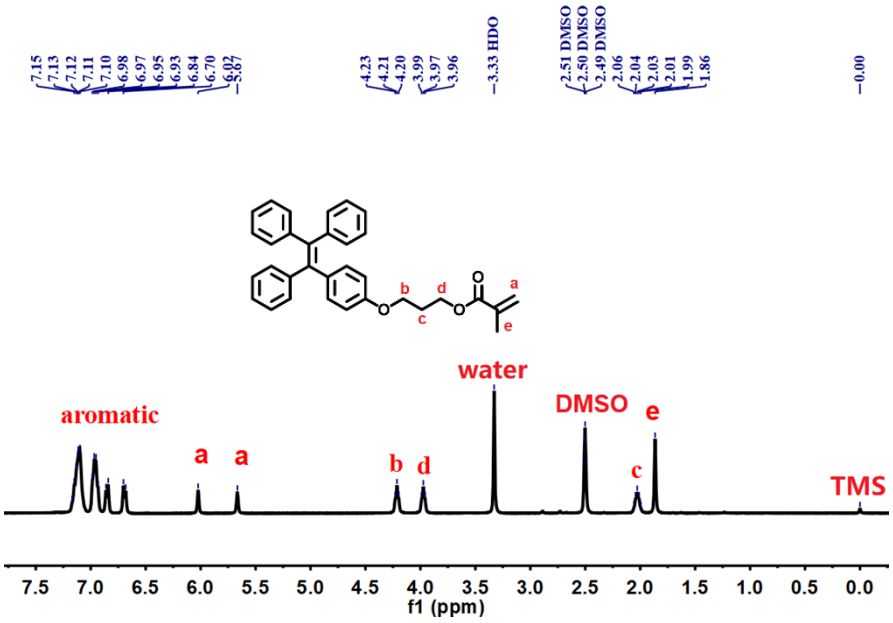

Fig. S6 ^{1}H NMR spectrum of TPE-MA in DMSO-d_6

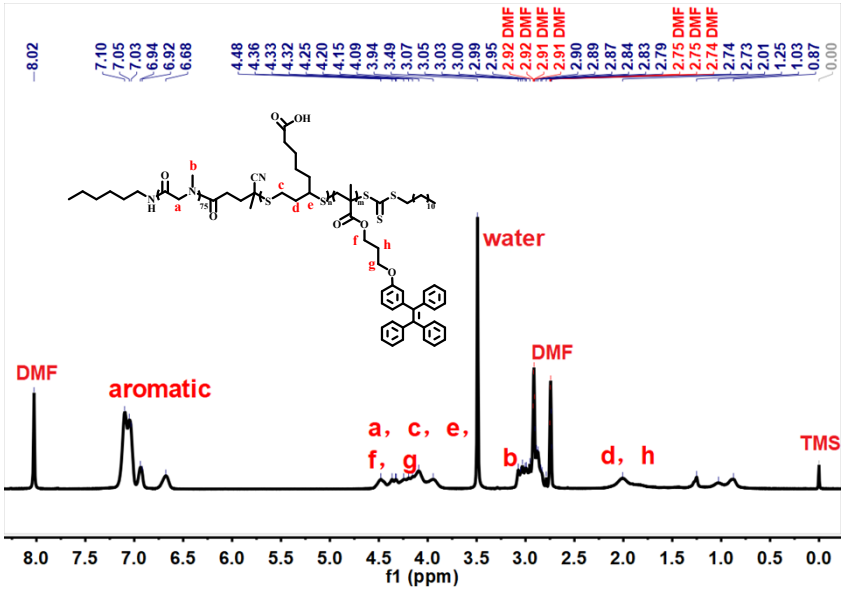

Fig. S7 ^{1}H NMR spectrum of Psar-b-P(LA-co-TPE) in DMF-d_7

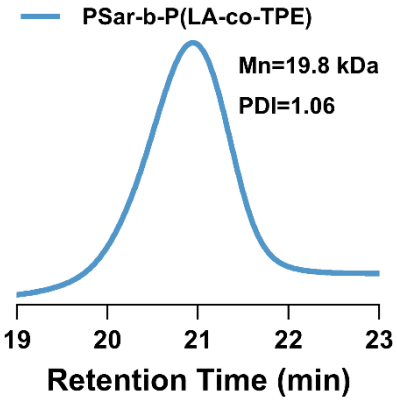

Fig. S8 The GPC curve of Psar-b-P(LA-co-TPE).

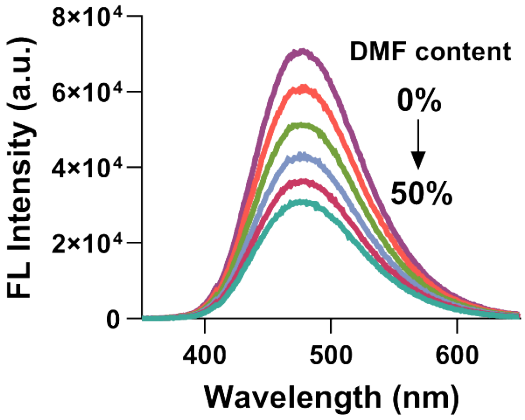

Fig. S9 Fluorescence of Psar-b-(LA-co-TPE) in different concentrations of DMF.

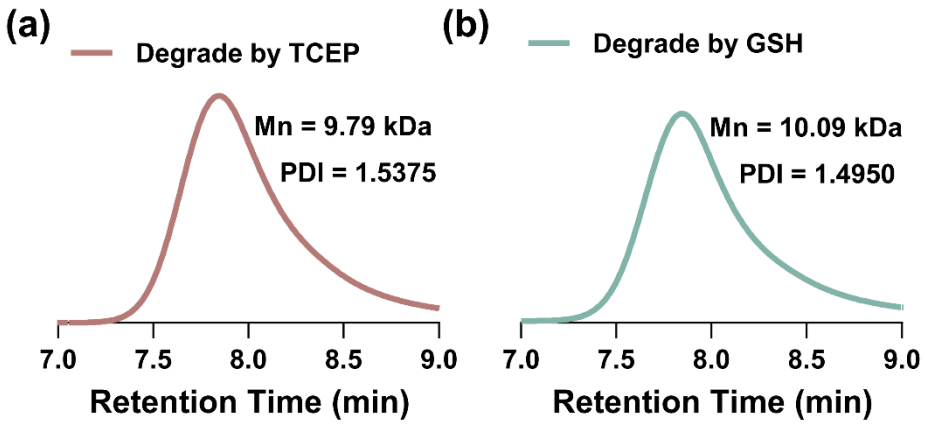

Fig. S10 The GPC curve of Psar-b-P(LA-co-TPE) degradation products by (a) TCEP and (b) GSH, respectively. The concentrations of TCEP and GSH were both 5 mM, with an incubation time of 30 minutes.

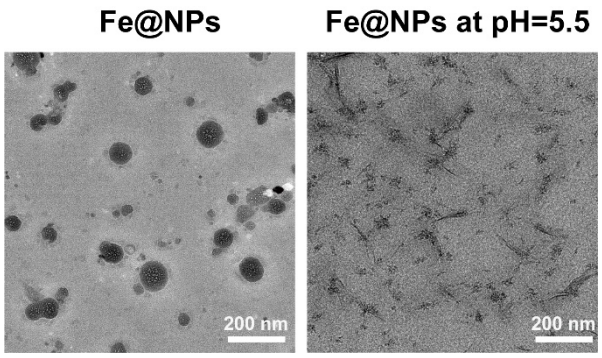

Fig. S11 TEM images of Fe@NPs in PBS 7.4 and PBS 5.5.

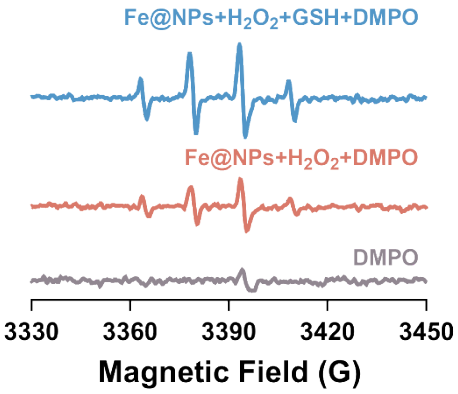

Fig. S12 The EPR analysis of Fe@NPs in different conditions (the concentration of H_2O_2 or GSH is 5 mM).

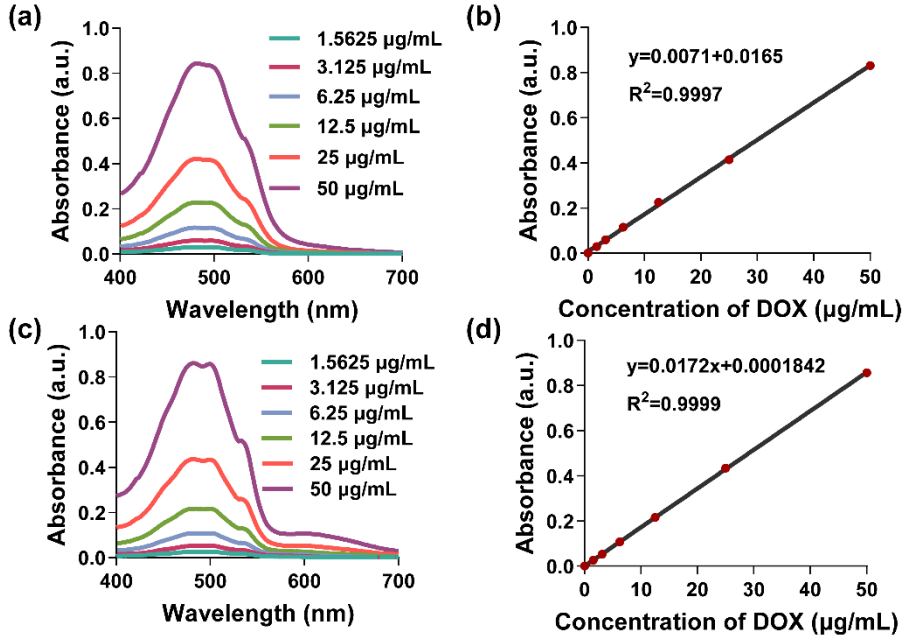

Fig. S13 (a) UV-Vis absorption curves of DOX with different concentrations in water. (b) Standard curve of DOX in water. (c) UV-Vis absorption curves of DOX with different concentrations in DMSO. (d) Standard curve of DOX in DMSO.

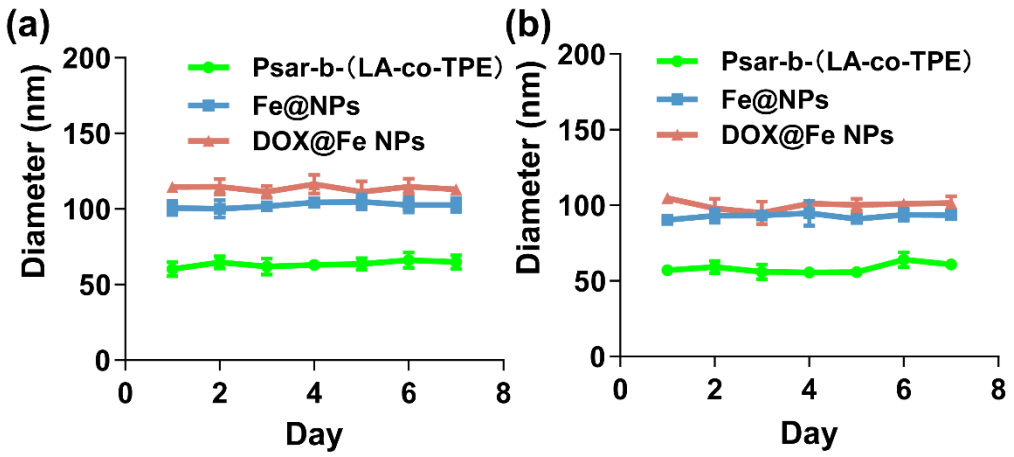

Fig. S14 Change of diameters of Psar-b-P(LA-co-TPE) NPs, Fe@NPs, and DOX@FeNPs in H_2O (a) and DMEM (b).

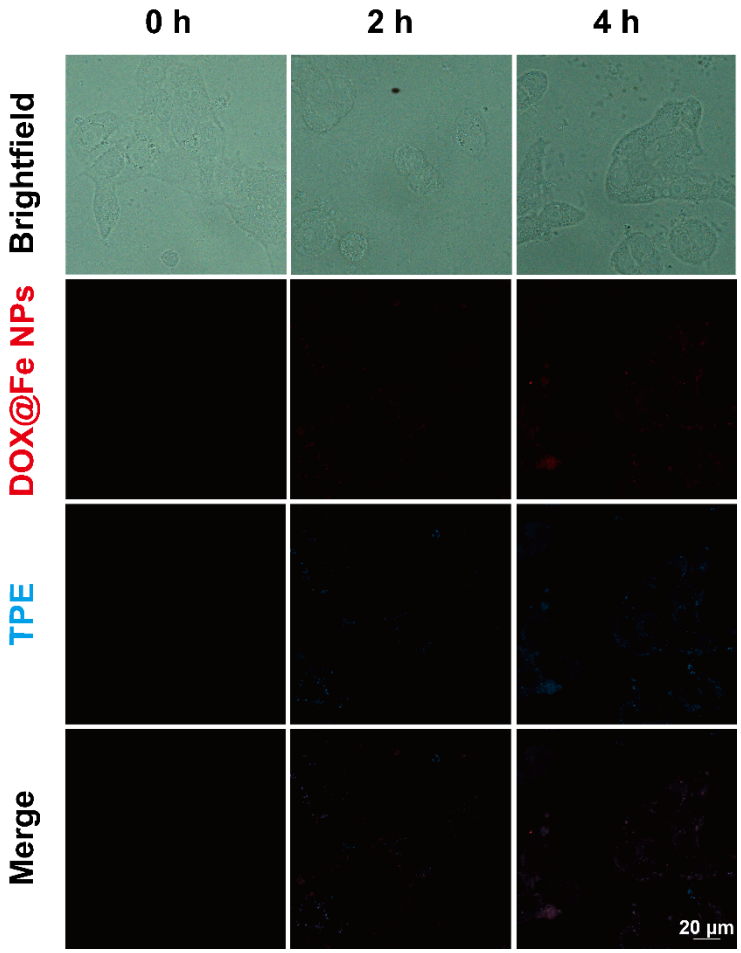

Fig. S15 The cellular uptake of DOX@Fe NPs at 4°C. (scale bar 20 μm)

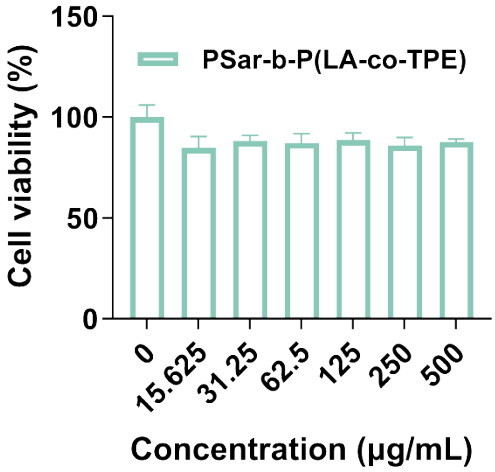

Fig. S16 Cell viability of Psar-b-P(LA-co-TPE) against 4T1 cells.